NJC

PAPER

View Article Online
View Journal | View Issue

Cite this: *New J. Chem.*, 2025, **49**, 8225

An infinite 2D sheet of tetragonal Co^{II} framework exhibiting metamagnetism†

Arindam Gupta, [a] Pramod Bhatt *[bc] and Sanjit Konar *[a]

Received 11th January 2025,
Accepted 8th April 2025

DOI: 10.1039/d5nj00157a

rsc.li/njc

A two-dimensional coordination polymer $[Co(pyz)(CA)]_n$ (complex **1**) was synthesized and structurally characterized. Solid-state dc magnetic susceptibility revealed overall antiferromagnetic interactions in the complex with an antiferromagnetic ordering below 7 K (Néel temperature, T_N). Magnetization measurements revealed a sigmoidal nature indicative of metamagnetic behaviour, with an abrupt increase in magnetization at 4.7 T. Variable field susceptibility studies indicated a magnetic phase transition, marked by a cusp at 11 K that disappeared at fields above 0.05 T. Hydrostatic pressure decreased the overall magnetic moment without altering the T_N or the hysteresis width. Broken-symmetry density functional theory (BS-DFT) calculations indicated antiferromagnetic interactions between Co^{II} ions mediated by pyrazine and chloranilate anions, and also emphasized the significant role of easy-axis anisotropy of the Co^{II} ion in the metamagnetic behaviour in complex **1**.

Introduction

Molecule-based magnets exhibit intriguing physical phenomena like spin frustration, spin-canting, metamagnetism, and ferrimagnetism, which help us comprehend the origin of these fundamental phenomena at the molecular level.[1–6] Thus, infinite layer-type structures like 1D chains, 2D sheets, and 3D frameworks are of interest to scientists owing to their fascinating structural diversity and potential functions as low-dimensional magnetic materials.[4,5] The crystal engineering of molecule-based coordination frameworks goes hand-in-hand with explaining the fundamentals of magnetism in the frameworks.[5,6] The design of coordination polymers requires the proper choice of metal centres and the bridging ligands capable of transmitting exchange interactions between the metal centres must be appropriate.[3,6] Indeed, designing low-dimensional magnetic materials requires careful choice of metal ions and bridging ligands to achieve the desired magnetic anisotropy and exchange coupling properties.[1,2,5,7–13] In magnetic systems, competing exchange interactions are at the heart of the complex and emergent magnetic phenomena, often leading to frustration, exotic ground states, and unconventional magnetic phenomena.

Metamagnetism is a phenomenon that is rarely observed and occurs when net magnetic moments get aligned in antiparallel directions by weak antiferromagnetic interactions that are mostly secondary and can be overcome by applying a large external field, thereby generating ferro-, ferri-, or weak ferromagnetic states in the material.[1,2,7,14,15] The application of a magnetic field rotates the magnetization perpendicular to the magnetic field, generating two types of metamagnetic transition, depending upon the strength of the magnetocrystalline anisotropy: spin–flip and spin–flop.[16] A large anisotropic system leads to spin-canting through possible antisymmetric superexchange interactions and may induce metamagnetic transition (usually spin–flip), whereas a small anisotropy in the system causes spin–flop to occur.[17–19] Although spin-canting, spin–flop, and metamagnetism behave differently in the presence of a magnetic field, they share common features, such as the significant role of magnetic anisotropy in their exhibition.[1,2,7,20,21]

Weak metamagnetic transition was observed in an azido-bridged Mn^{II} complex $[Mn(tptz)(\mu_{1,1}\text{-}N_3)_2]_n$ [tptz = 2,4,6-tris(2-pyridyl)-1,3,5-triazine], possessing a 2D sheet-like structure.[2] Magnetic analyses revealed weak interchain antiferromagnetic interactions and dominant intrachain ferromagnetic interactions *via* an end-on (EO) azide-bridge, thereby giving rise to overall metamagnetic behavior having 3D magnetic ordering at 2.7 K and a critical field of 8 mT, at which the interlayer antiferromagnetic ground-state switched to a ferromagnetic one. Another 2D coordination network bearing the molecular formula $[Co(N_3)_2(ampyz)]_n$ (ampyz = 2-aminopyrazine) possessing a 1D chain of alternately double EO and double end-to-end (EE) azido-bridged Co^{II} ions with the ampyz ligands occupying the trans-positions of Co^{II} was found to exhibit metamagnetic transition having a critical field of 60 mT and magnetic ordering

[a] *Department of Chemistry, Academic Building 2, Indian Institute of Science Education and Research Bhopal, Bhopal By-pass road, Bhauri, Madhya Pradesh-462 066, India. E-mail: skonar@iiserb.ac.in*
[b] *Solid State Physics Division, Bhabha Atomic Research Centre, Mumbai-400085, India. E-mail: prabhatt@barc.gov.in*
[c] *Homi Bhabha National Institute, Anushaktinagar, Mumbai 400 094, India*

† Electronic supplementary information (ESI) available. CCDC 2258079. For ESI and crystallographic data in CIF or other electronic format see DOI: https://doi.org/10.1039/d5nj00157a

below 11 K.[22] Metamagnetism coupled with antiferromagnetic phase transition at 12 K and 200 Oe dc field was observed for 1D doubly bridged-azido-cobalt(II) complex *catena*-{[Co($\mu_{1,1}$-N_3)$_2$(H_2O)$_2$]-(3-picoline-*N*-oxide)$_2$} (3-picoline-*N*-oxide = 3-methylpyridine-*N*-oxide). Intrachain ferromagnetic coupling was observed between the Co^{II}-centres *via* azide moieties together with weak interchain antiferromagnetic coupling resulting in the metamagnetic transition.[23]

Our strategy involved synthesizing a 2D coordination polymer using a mixed-ligand approach that assembles the anisotropic metal ion at the nodes of a tetragonal lattice, generating effective magnetic coupling through both ligands to achieve magnetic ordering. The molecular formula of the complex is $[Co(CA)(pyz)]_n$ (CA = chloranilate anion, pyz = pyrazine), which exhibited two types of antiferromagnetic exchange interactions ($J = -0.32$ cm^{-1} and $zJ' = -0.34$ cm^{-1}).[24] The presence of two types of magnetic exchange coupling within the complex prompted an investigation into the potential for spin canting and metamagnetism. Field-cooled and zero-field-cooled DC magnetic susceptibility measurements diverged below 7 K, indicating the presence of magnetic ordering and spin canting. The sigmoidal nature of the magnetization data primarily confirmed the metamagnetic behaviour in the complex. The complex also exhibited a magnetic phase transition, as revealed by variable magnetic field data, where a cusp observed at 7 K at lower fields disappeared at fields exceeding 500 Oe. Density functional theory calculations supported the antiferromagnetic exchange coupling parameters, established the exchange coupling occurring *via* pyrazine as well as chloranilate anions and the role of easy-axis anisotropy of the Co^{II} ion on the metamagnetic behaviour of the complex.

Results and discussion

Single-crystal X-ray diffraction

Complex **1** (CCDC 2258079) crystallizes in centrosymmetric monoclinic space group *C*2/*m* and the asymmetric unit consists of a Co^{II} ion, half of a chloranilate anion, and one-third of pyrazine. The crystallographic table has been provided in Table S1, ESI.† The Co^{II} ion is in a slightly distorted [CoN_2O_4] octahedral environment OC-6 (CShM 0.823) as calculated from SHAPE (Fig. 1a and Table S2, ESI†). The structure can be best described as an infinite square array where a pyrazine moiety is bonded to a Co^{II} ion axially that extends along the crystallographic *b* axis, whereas a chloranilate anion gets bonded to the Co^{II} ion equatorially and extends along the crystallographic *c* axis (Fig. 1b). The Co^{II} ions along with the chloranilate anions sit on the mirror plane, and the line connecting metal and N-atoms of pyrazine coincides with the crystallographic two-fold axis perpendicular to the mirror plane, and the Co–N bonds are perpendicular to the CA^{2-} plane. The ⟨Co–N⟩ and ⟨Co–O⟩ bond lengths are 2.199 Å and 2.0755 Å. The two types of C–O bond lengths 1.279 Å and 1.238 Å depict the dinegative character of the chloranilate anion. Furthermore, the C–C bond lengths of 1.364 Å, 1.395 Å, and 1.546 Å confirm the above observation. The nearest Co–pyz–Co and Co–CA–Co distances are 7.192 Å and 7.916 Å, respectively. Two types of C–H···O interactions have been observed between the C–H atoms of pyrazine and the O atoms of the chloranilate anion, one intralayer (2.456 Å) and the other interlayer (2.503 Å) (Fig. S1a, ESI†). The packing of complex **1** along the crystallographic *ab* plane has been shown in Fig. S1b, ESI.†

Magnetic studies

The phase of the crystalline and powder samples of complex **1** has been confirmed from the powder X-ray diffraction data (Fig. S2, ESI†). DC magnetic susceptibility of complex **1** was collected on microcrystalline samples at 0.1 T dc magnetic field. The room temperature $\chi_M T$ value of complex **1** is 3.12 cm^3 K mol^{-1}, higher than the spin-only value for one isolated Co^{II} ion (1.87 cm^3 K mol^{-1}, $S = 3/2$). With decreasing temperature, the susceptibility value decreased to 0.16 cm^3 K mol^{-1} at 2 K owing to the antiferromagnetic interactions between Co^{II} ions *via* the pyrazine and chloranilate anion as well as due to the zero-field splitting of the Co^{II} ion (Fig. 2).

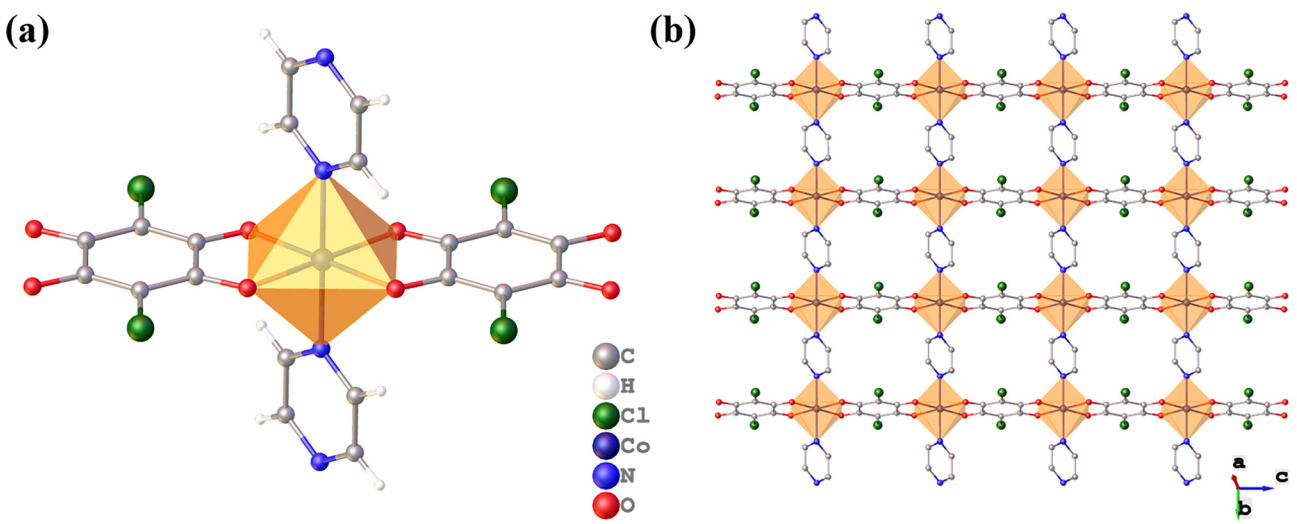

Fig. 1 (a) Monomer unit of complex **1**, and (b) view of the 2D sheet along the crystallographic *bc* plane.

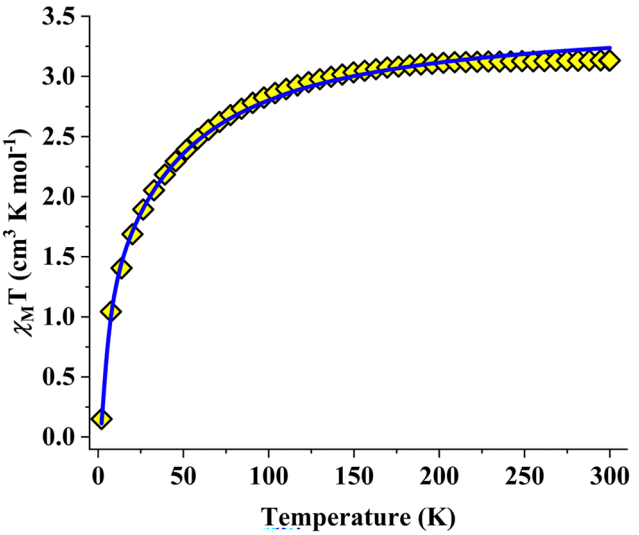

Fig. 2 DC magnetic susceptibility of complex **1**. The yellow rhombus and the blue line indicate experimental data and fitting using the equation proposed by Rueff *et al.*, respectively.

Fitting of the χ_M^{-1} *vs.* T plot above 100 K gives Curie constant C = 3.28 cm^3 K mol^{-1} and a Weiss constant $\theta = -12.98$ K (Fig. S3, ESI†). The negative Weiss constant can be attributed to the antiferromagnetic interaction between the Co^{II} ions *via* pyrazine and chloranilate anions and significant spin–orbit coupling of the octahedral Co^{II} ions having ground term $^4T_{1g}$. The magnetic susceptibility data was fitted by the equation proposed by Rueff *et al.* for a low-dimensional antiferromagnetic Co^{II} complex that can predict the extent of antiferromagnetic interaction and spin–orbit coupling.[6,25] The equation is $\chi_M T = A\exp(-E_1/kT) + B\exp(-E_2/kT)$, where $A + B$ equals the Curie constant, and E_1 and E_2 represent the activation energies for spin–orbit coupling for the Co^{II} ion and overall antiferromagnetic exchange interaction between Co^{II} ions, respectively. According to the Ising chain approximation, magnetic exchange interaction (J) can be related to E_2 as $\chi_M T \propto \exp(+J/2kT)$. The fitted parameters are $A + B$ = 3.5 cm^3 K mol^{-1}, equivalent to the Curie constant obtained from fitting the χ_M^{-1} *vs.* T plot in the high-temperature range. The $-E_1/k$ is −41.07 (0.21) cm^{-1}, which has been found for other Co^{II} complexes reported earlier.[25,26] The overall antiferromagnetic coupling E_2/k = +4.13 (0.03) cm^{-1} corresponds to $J = -8.27$ cm^{-1}, close to values reported earlier for 2D antiferromagnets.

To verify whether any magnetic ordering exists in complex **1**, field-cooled and zero-field-cooled magnetic susceptibility was measured at 100 Oe dc field. Disagreement was shown between the FC and ZFC plots below 7 K (Néel temperature T_N), thereby suggesting the onset of antiferromagnetic ordering and hysteretic long-range magnetic order below T_N (Fig. 3a). To confirm the occurrence of magnetic ordering, ac susceptibility measurements were carried out in an alternating field of 3.5 Oe at a frequency range of 1–600 Hz. The maximum of χ' is observed at T_N = 7 K (Fig. S4a, ESI†). The presence of an unclear peak maxima in the χ'' plot below 7 K confirms the canted antiferromagnetic nature of complex **1** (Fig. S4b, ESI†), having no frequency dependency.[18] Furthermore, the field dependence behaviour of the field-cooled

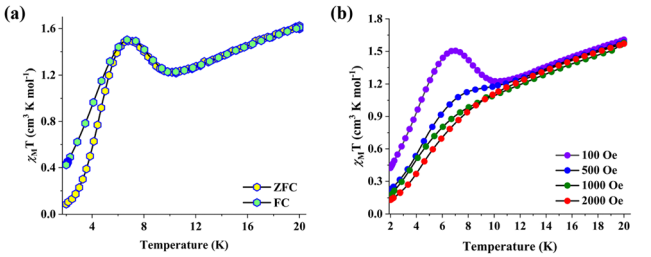

Fig. 3 (a) FC-ZFC plot of complex **1** collected at 100 Oe dc field, and (b) dc magnetic susceptibility collected at variable dc field below 20 K.

magnetization for complex **1** was studied by varying the magnetic field below T_N. At a lower field (100 Oe), there appears to be a cusp at around 7 K (Fig. 3b and Fig. S5, ESI†). The cusp observed in the magnetic susceptibility of complex **1** at 0.01 T indicates a very weak magnetized state owing to spin canting, thereby leading to an increase in the magnetic moment. As the dc magnetic field increases, the cusp vanishes, indicating the disruption of the spin canting and the reorientation of the spins resulting in a purely antiferromagnetic state.[27,28]

The magnetization *versus* field curves at 2 K, 4 K, and 6 K show sigmoidal nature, indicative of typical metamagnetic behaviour, and do not saturate at 7 T, the value being 1.86μ_B (at 2 K) and it depicts the strong antiferromagnetic coupling between Co^{II} ions in complex **1** (Fig. 4a). At fields below the critical field $H_C \approx 4.7$ T (the maximum obtained in the $\partial M/\partial H$ plot at 2 K), the magnetization increases linearly, indicating the presence of antiferromagnetic interactions. Beyond this point, a sharp increase in the magnetization up to 7 T is observed, characteristic of metamagnetic behaviour and suggestive of a field-induced spin reorientation, thereby leading to a paramagnetic state. The absence of saturation (S' = 1/2, g' = 4.33, M_s = 2.16μ_B for octahedral Co^{II} at 2 K) in the magnetization at higher fields indicates an incomplete suppression of antiferromagnetic coupling. The reduced magnetization plot shows a non-superimposable nature, indicating significant anisotropy in complex **1** (Fig. 4b). A hysteresis loop has been observed at fields lower than 1 T, yielding a coercive field of ∼525 Oe with a remanent magnetization M_r of ∼0.00135μ_B at 2 K (Fig. S6, ESI†). The hysteresis loop closes at 5 K, the coercive field being ∼26 Oe and remanent magnetization of ∼4.3 × 10$^{-4}\mu_B$. This is indicative of the formation of residual spins resulting from the

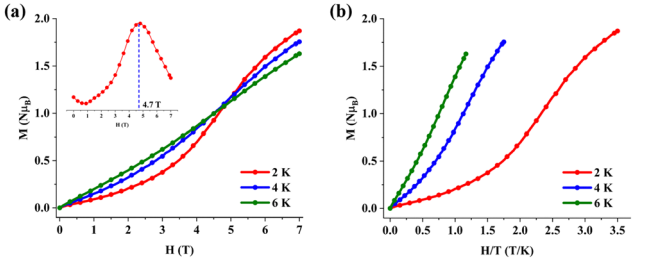

Fig. 4 Magnetization *vs.* field plot (a) and reduced magnetization *vs.* field plot (b) of complex **1**. The derivative curve of the magnetization *vs.* field curve at 2 K is shown in the inset of (a).

spin canting effect of the antiferromagnetically coupled Co^{II} ions. These combined behaviours confirm the occurrence of spin-canted antiferromagnetism and metamagnetism. The spin canting angle (α) is estimated to be $\sim 0.16^{\circ}$, calculated using the equation: $\alpha = \sin^{-1}(M_r/M_s)$, M_s being $2.16\mu_B$ for octahedral Co^{II} at 2 K. The spin canting being small reflects the overall antiferromagnetic nature of complex **1** possessing a very weak magnetized state, as observed from the variable dc field magnetic susceptibility.

Neutron diffraction studies

To get an insight into the magnetic ordering, temperature-dependent neutron powder diffraction and depolarization measurements were performed. The fitted neutron diffraction data at 300 K confirms the single crystalline phase of complex **1** having a monoclinic crystal structure of space group C2/*m* (Table S3, ESI†). The intensities and positions of the Bragg peaks for neutron diffraction data at 25 K did not change as compared to the neutron diffraction data at 300 K and confirm the paramagnetic nature of complex **1** (Fig. 5a and b). The Rietveld refined neutron diffraction data recorded at 5 K does not show any additional peaks or enhancement in the intensities of the fundamental nuclear Bragg peaks, confirming the absence of long-range ordering present in the compound down to 5 K. This could be possible because the lowest possible neutron diffraction measurement temperature (5 K) is close to the ordering temperature of the compound. Furthermore, the presence of background due to the hydrogen atoms makes the signals subtle.[29,30] The temperature-dependent neutron depolarization of complex 1 shows no depolarization of the neutron beam down to 3.5 K, further confirming the absence of ferromagnetic or ferrimagnetic domains/clusters under an applied field of 10 Oe.

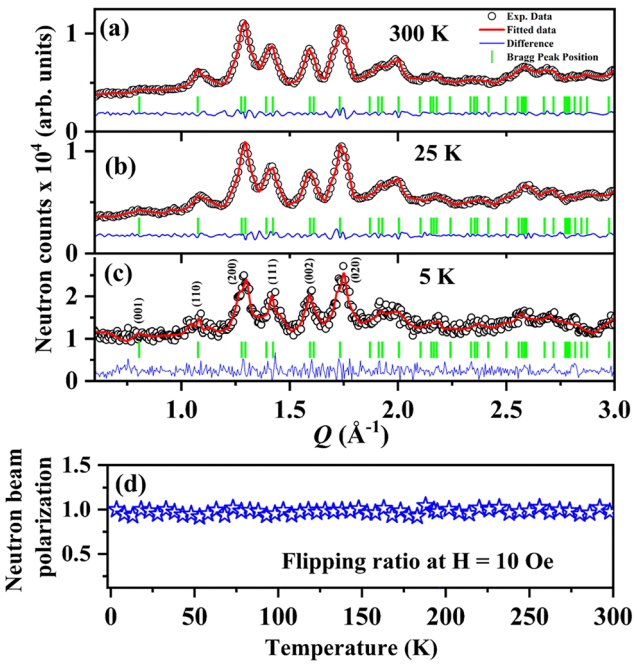

Fig. 5 The Rietveld refined neutron diffraction patterns of complex **1** at various temperatures (a)–(c). The experimental and simulated data have been represented with open circles and solid lines, respectively. Solid lines at the bottom show the difference between experimental and fitted patterns. Temperature-dependent neutron depolarization of complex **1** at 10 Oe.

Pressure-induced dc magnetic studies

Although chemical tuning of magnetic ordering by doping has been studied, physical tuning of magnetic phenomena is still an area of active exploration.[31,32] Among the physical stimuli, tuning magnetic ordering using hydrostatic pressure is particularly intriguing. While the ordering temperature is generally pressure-independent, the metamagnetic transitions show significant pressure dependence.[33] Increasing hydrostatic pressure reduces the interlayer distance, thereby enhancing the effective magnetic coupling between the metal centers and hence, the competition between the exchange interactions. To get an insight into the effect of hydrostatic pressure on the spin canting and metamagnetic behaviour of complex **1**, dc magnetic susceptibility was studied on powdered samples by applying hydrostatic pressures of 0 GPa and 1 GPa. Increasing the hydrostatic pressure does not alter the T_N; however, the magnetic moment (χ_M) at 7 K decreased from 0.41 $cm^3\ mol^{-1}$ (0 GPa) to 0.34 $cm^3\ mol^{-1}$ (1 GPa) (Fig. 6a and Fig. S7, ESI†). This suggests that while the applied pressure did not alter the nature and temperature of the antiferromagnetic ordering as anticipated, it reduced the magnetic moment, likely due to some of the Co^{II} ions undergoing HS to LS conversion upon application of pressure. The sigmoidal nature of the magnetization *versus* field

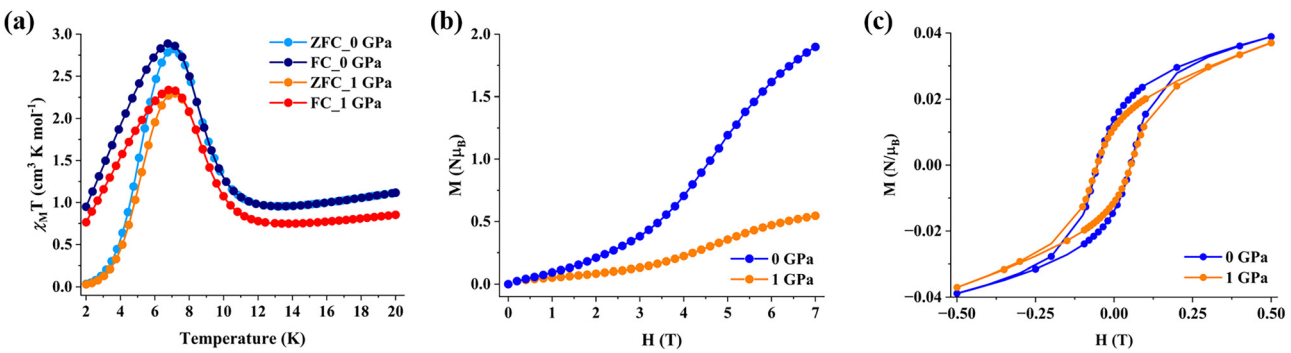

Fig. 6 FC-ZFC plot at 100 Oe dc field (a), magnetization *vs.* field plot at 2 K (b), and hysteresis plot at 2 K (c) at 0 GPa and 1 GPa hydrostatic pressure, respectively.

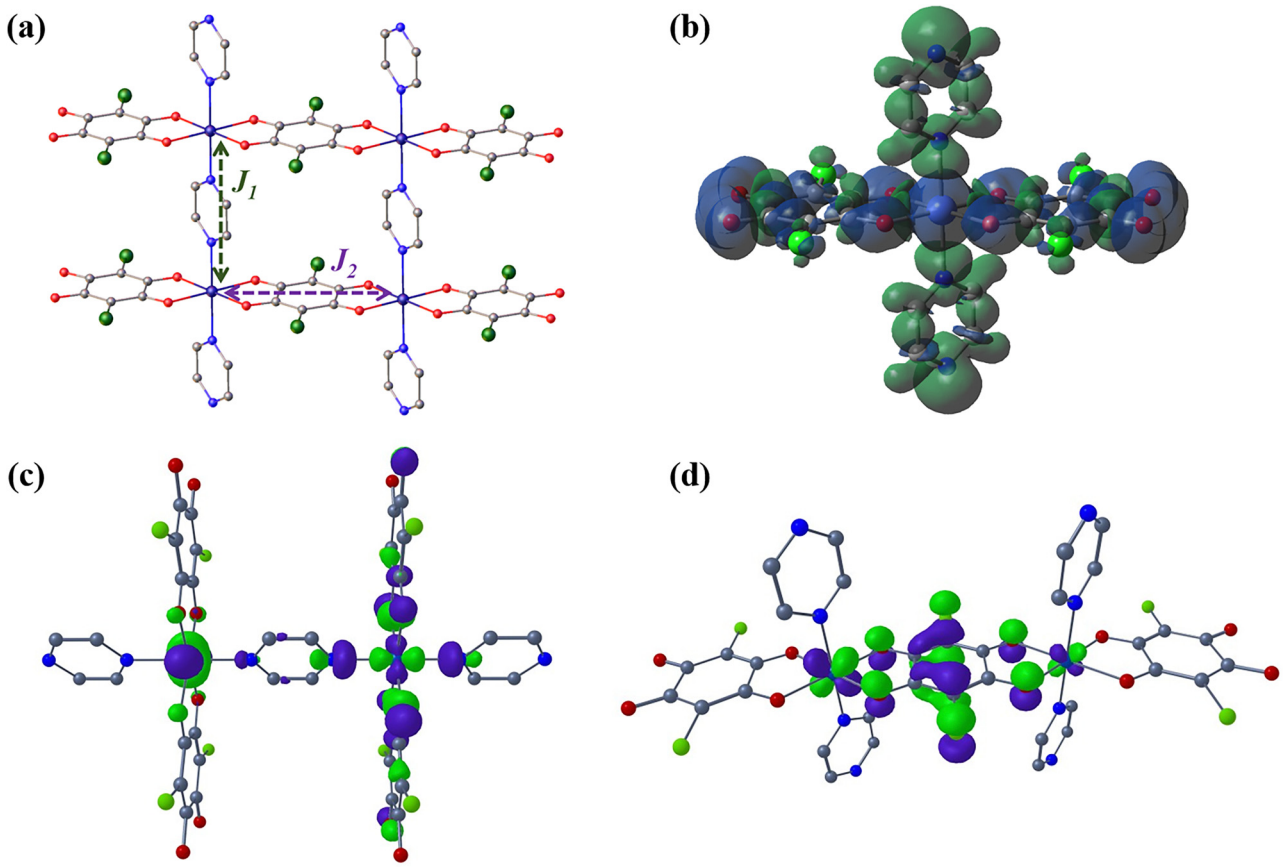

Fig. 7 (a) Scheme showing exchange coupling parameters (J_1 and J_2); (b) spin density plot showing the delocalization of electrons throughout the framework atoms; involvement of the d_{z^2} and $d_{x^2-y^2}$ orbitals of Co^{II} ions in exchange coupling *via* pyrazine (c), and the d_{yz} orbitals of neighbouring Co^{II} ions in coupling with chloranilate ions (d).

curve was preserved even upon the application of 1 GPa pressure; however, the magnetization value decreased from 1.8μ_B (0 GPa) to 0.55μ_B (1 GPa) (Fig. 6b). The nature of the hysteresis curve remained unchanged, with the coercive field remaining at 525 Oe. However, the remanent magnetization reduced from 0.0135μ_B at 0 GPa to 0.011μ_B at 1 GPa (Fig. 6c).

Theoretical studies

To elucidate whether the antisymmetric exchange or magnetic anisotropy is responsible for the observed metamagnetic behaviour of complex **1**, the magnetic exchange coupling and the interacting magnetic orbitals involved were further analyzed by BS-DFT calculations performed in the ORCA 5.0.3 software package.[34] Two types of exchange coupling have been computed, one *via* pyrazine (J_1) and the other *via* a chloranilate anion (J_2) (Fig. 7a). BS-DFT calculations yielded $J_1 = -0.23$ cm^{-1} and $J_2 = -2.49$ cm^{-1} as per equation **1**,[35,36] which matches well with the experimentally fitted data.

$$J = \frac{-(E_{HS} - E_{BS})}{\langle S_{HS}{}^2\rangle - \langle S_{BS}{}^2\rangle}$$

where, J, E_{HS}, E_{LS}, S_{HS}, and S_{LS} denote the exchange coupling constant, the energy of the triplet state, the energy of the singlet state, and overall spin of the high spin and low spin state, respectively. Since, both the exchange couplings are antiferromagnetic, the anisotropy of the Co^{II} ion may play a pivotal role in the observation of metamagnetic behaviour in complex **1**.

Visualization of the magnetic orbitals shows the involvement of d_{z^2} and $d_{x^2-y^2}$ orbitals of adjacent Co^{II} ions *via* pyrazine, whereas the d_{yz} orbitals of neighbouring Co^{II} ions participate in magnetic coupling *via* the chloranilate anion (Fig. 7c and d). Spin density calculations show substantial negative electron density on both the pyrazine and chloranilate anion, thereby suggesting exchange coupling *via* both the bridging ligands (Fig. 7b). Furthermore, the Mulliken charge density on the O-atoms of the chloranilate anions (−0.2145) is greater than that of the N-atoms of pyrazine (−0.083), thereby indicating stronger magnetic coupling between the Co^{II} ions *via* the chloranilate anion (Fig. S8, ESI†).

The AILFT computed anisotropy parameter $D = -123.28$ cm^{-1} and $E/D = 0.27$ is consistent with the easy-axis anisotropy of the Co^{II} ion; however, ORCA highly overestimated the D-value. The g-values of $g_x = 1.06$, $g_y = 1.59$, and $g_z = 3.29$ ($g_{iso} = 1.98$), also support the easy-axis anisotropy of the Co^{II} ion.

Conclusions

The complex $[Co(pyz)(CA)]_n$ exhibits metamagnetism, supported by a sigmoidal magnetization curve with a critical field

of 4.7 T. It undergoes a magnetic phase transition, indicated by a cusp at T_N ~7 K, which disappears under higher magnetic fields. The fitting of the magnetic susceptibility data suggests the anisotropy of the Co^{II} ion as a potential cause for the observed metamagnetic behaviour. Neutron diffraction shows no change in the intensity of the Bragg peaks throughout the temperature range, indicating the absence of magnetic ordering. Hydrostatic pressure does not alter the antiferromagnetic ordering or metamagnetic transition but reduces the magnetic moment, likely due to an HS to LS conversion of some Co^{II} ions. BS-DFT calculations indicate antiferromagnetic exchange interactions between Co^{II} ions *via* pyrazine and chloranilate anions, which contribute minimally to the metamagnetic behavior, with the easy-axis anisotropy dictating the metamagnetic behaviour of the complex.

Author contributions

A. G. has performed the experiments. P. B. has performed the neutron diffraction studies. The data were interpreted by A. G. and S. K. The manuscript was written through the contributions of all the authors. All authors have given approval to the final version of the manuscript.

Data availability

The data supporting this article have been included as part of the ESI.†

Conflicts of interest

There are no conflicts to declare.

Acknowledgements

S. K. and A. G. are thankful to IISER Bhopal for the instrumentation and HPC facilities. A. G. is thankful to IISER Bhopal for the senior research fellowship. The research of the manuscript has been funded by BRNS (Project No. 58/14/08/2021-BRNS/37101) and MoE STARS (Project No. STARS-2/2023-0301).

Notes and references

1 X.-Y. Wang, L. Wang, Z.-M. Wang, G. Su and S. Gao, *Chem. Mater.*, 2005, **17**, 6369–6380.
2 A. Das, G. M. Rosair, M. S. El Fallah, J. Ribas and S. Mitra, *Inorg. Chem.*, 2006, **45**, 3301–3306.
3 H. H. Ko, J. H. Lim, H. C. Kim and C. S. Hong, *Inorg. Chem.*, 2006, **45**, 8847–8849.
4 S. Konar, P. S. Mukherjee, E. Zangrando, F. Lloret and N. R. Chaudhuri, *Angew. Chem., Int. Ed.*, 2002, **41**, 1561–1563.
5 S. Konar, S. Dalai, J. Ribas, M. G. B. Drew, E. Zangrando and N. Ray Chaudhuri, *Inorg. Chim. Acta*, 2004, **357**, 4208–4214.
6 J. Boonmak, M. Nakano and S. Youngme, *Dalton Trans.*, 2011, **40**, 1254–1260.
7 C. S. Hong and Y. Do, *Angew. Chem., Int. Ed.*, 1999, **38**, 193–195.
8 J. Yadav, A. Gupta, A. Mondal, F. Daumann, G. Hörner, B. Weber and S. Konar, *Chem. – Eur. J.*, 2024, **30**, e202400321.
9 Y. Wang, M. E. Ziebel, L. Sun, J. T. Gish, T. J. Pearson, X.-Z. Lu, A. E. Thorarinsdottir, M. C. Hersam, J. R. Long, D. E. Freedman, J. M. Rondinelli, D. Puggioni and T. D. Harris, *Chem. Mater.*, 2021, **33**, 8712–8721.
10 L. Liu, J. A. DeGayner, L. Sun, D. Z. Zee and T. D. Harris, *Chem. Sci.*, 2019, **10**, 4652–4661.
11 J. A. DeGayner, I.-R. Jeon, L. Sun, M. Dincă and T. D. Harris, *J. Am. Chem. Soc.*, 2017, **139**, 4175–4184.
12 G. Viau, M. Grazia Lombardi, G. De Munno, M. Julve, F. Lloret, J. Faus, A. Caneschi and J. Modesto Clemente-Juan, *Chem. Commun.*, 1997, 1195–1196, DOI: 10.1039/A701219E.
13 Y.-Z. Zhang, S. Gao, H.-L. Sun, G. Su, Z.-M. Wang and S.-W. Zhang, *Chem. Commun.*, 2004, 1906–1907, DOI: 10.1039/B405167J.
14 J.-Y. Zou, W. Shi, H.-L. Gao, J.-Z. Cui and P. Cheng, *Inorg. Chem. Front.*, 2014, **1**, 242–248.
15 S. Akagi, J. Wang, K. Imoto, K. Kumar, S.-I. Ohkoshi and H. Tokoro, *Pure Appl. Chem.*, 2023, **95**, 701–705.
16 B. Leclercq, H. Kabbour, F. Damay, C. V. Colin, A. Pautrat, A. M. Arevalo-Lopez and O. Mentré, *Inorg. Chem.*, 2019, **58**, 12609–12617.
17 R. L. Carlin and A. Van Duyneveldt, *Acc. Chem. Res.*, 1980, **13**, 231–236.
18 M.-H. Zeng, W.-X. Zhang, X.-Z. Sun and X.-M. Chen, *Angew. Chem., Int. Ed.*, 2005, **44**, 3079–3082.
19 Y.-Q. Tian, C.-X. Cai, X.-M. Ren, C.-Y. Duan, Y. Xu, S. Gao and X.-Z. You, *Chem. – Eur. J.*, 2003, **9**, 5673–5685.
20 Y. S. You, J. H. Yoon, H. C. Kim and C. S. Hong, *Chem. Commun.*, 2005, 4116–4118, DOI: 10.1039/B507051A.
21 C. S. Hong, J.-e Koo, S.-K. Son, Y. S. Lee, Y.-S. Kim and Y. Do, *Chem. – Eur. J.*, 2001, **7**, 4243–4252.
22 J. Boonmak, M. Nakano, N. Chaichit, C. Pakawatchai and S. Youngme, *Inorg. Chem.*, 2011, **50**, 7324–7333.
23 F. A. Mautner, C. Berger, R. C. Fischer, S. S. Massoud, S. Speed and R. Vicente, *Polyhedron*, 2019, **170**, 622–629.
24 H. Kumagai, S. Kawata and S. Kitagawa, *Inorg. Chim. Acta*, 2002, **337**, 387–392.
25 J.-M. Rueff, N. Masciocchi, P. Rabu, A. Sironi and A. Skoulios, *Chem. – Eur. J.*, 2002, **8**, 1813–1820.
26 J.-M. Rueff, N. Masciocchi, P. Rabu, A. Sironi and A. Skoulios, *Eur. J. Inorg. Chem.*, 2001, 2843–2848.
27 J. Pasán, J. Sanchiz, C. Ruiz-Pérez, J. Campo, F. Lloret and M. Julve, *Chem. Commun.*, 2006, 2857–2859, DOI: 10.1039/B602144A.
28 W.-W. Sun, C.-Y. Tian, X.-H. Jing, Y.-Q. Wang and E.-Q. Gao, *Chem. Commun.*, 2009, 4741–4743, DOI: 10.1039/B904068D.
29 P. Bhatt, A. Kumar, C. Ritter and S. M. Yusuf, *J. Phys. Chem. C*, 2020, **124**, 19228–19239.
30 P. Bhatt, N. Maiti, M. D. Mukadam, S. S. Meena, A. Kumar and S. M. Yusuf, *Phys. Rev. B*, 2023, **108**, 014412.

31 W. Chen, Y. Hu, W. Lv, T. Lei, X. Wang, Z. Li, M. Zhang, J. Huang, X. Du, Y. Yan, W. He, C. Liu, M. Liao, W. Zhang, J. Xiong and C. Yan, *Nat. Commun.*, 2019, **10**, 4973.
32 C. Hu, S.-W. Lien, E. Feng, S. Mackey, H.-J. Tien, I. I. Mazin, H. Cao, T.-R. Chang and N. Ni, *Phys. Rev. B*, 2021, **104**, 054422.
33 T. Qian, E. Emmanouilidou, C. Hu, J. C. Green, I. I. Mazin and N. Ni, *Nano Lett.*, 2022, **22**, 5523–5529.
34 F. Neese, *Wiley Interdiscip. Rev.:Comput. Mol. Sci.*, 2022, **12**, e1606.
35 T. Soda, Y. Kitagawa, T. Onishi, Y. Takano, Y. Shigeta, H. Nagao, Y. Yoshioka and K. Yamaguchi, *Chem. Phys. Lett.*, 2000, **319**, 223–230.
36 K. Yamaguchi, Y. Takahara and T. Fueno, Dordrecht, 1986.